Soil Dynamics and Earthquake Engineering 184 (2024) 108846

Contents lists available at ScienceDirect

Soil Dynamics and Earthquake Engineering

journal homepage: www.elsevier.com/locate/soildyn

Pseudo-static approach for slope stability analysis within a stochastic probabilistic framework for moderate earthquakes

Pooneh Shah Malekpoor [a,*], Susana Lopez-Querol [a], Sina Javankhoshdel [b]

[a] Civil, Environmental and Geomatic Engineering, University College London (UCL), London, WC1E 6BT, UK
[b] Rocscience, Inc., 54 St. Patrick St., Toronto, ON, M5T 1V1, Canada

ARTICLE INFO

Keywords:
Slope stability
PS approach
Soil spatial variability
Random variability of input load
Non-circular RLEM

ABSTRACT

The routine pseudo-static (PS) approach does not consider the random variability of the seismic load which might lead to unconservative estimates of the slope failure probability in specific seismic regions and soil slopes. This research explores the effect of random variable PS loading in the stochastic slope stability analysis by employing the limit equilibrium method (LEM) of slices, Monte Carlo (MC) simulation and random field theory, termed 2D-RPSLEM. Results show the sensitivity of the problem to various factors, including different levels of uncertainty of the PS loading and the magnitude of the PS coefficient. In summary, it was observed that the inclusion of random variability for the PS coefficient leads to more conservative results for slopes with deterministic safety factors above 1.1 while resulting in lower risks for slopes with lower safety factors for larger magnitude seismic loads.

Nomenclature

Symbol	Description
μ_c	Mean cohesion
μ_ϕ	Mean friction angle
μ_{Kh}	Mean PS coefficient
Γ	Unit weight of soil
H	Slope height
λ $(=\mu_c/\gamma H tan\mu_\phi)$	Stability number
D	Depth factor
Δ_H	Horizontal coordinate of a point in the random field
Δ_V	Vertical coordinate of a point in the random field
ρ	Autocorrelation function
δ_H	Absolute horizontal distance between two locations within the random field
δ_V	Absolute vertical distance between two locations within the random field
θ_H	Horizontal scale of fluctuation (SoF)
θ_V	Vertical SoF
θ	Isotropic SoF
COV_c	Coefficient of variation of the soil cohesion
COV_ϕ	Coefficient of variation of the soil friction angle
COV_{Kh}	Coefficient of variation of the PS coefficient
$\theta_{c,\phi(H,V)}$	Isotropic SoF for the soil parameters
$\theta_{c,\phi(Ho)}$	Horizontal SoF for the soil parameters
$\theta_{c,\phi(V)}$	Vertical SoF for the soil parameters

1. Introduction and background studies

In earthquake engineering practice, slope stability is most frequently evaluated using the deterministic pseudo-static (PS) method, in which constant horizontal PS inertial forces are included in the safety factor calculations [1]. Of the primary requirements of the PS approach is that no significant cyclic strength degradation should occur in the material. The employed PS coefficients are usually based on literature values (i.e. Table 1). For example, Marcuson [2] believed that the PS coefficient, K_h, should be considered as (1/3–1/2)*PGA/g in the site where PGA is the amplified version of the peak bedrock acceleration (due to the design earthquake) measured at a critical point like the crest of an earth dam which was used for this particular analysis.

The values of the PS coefficient in Table 1 are often derived according to the calibration of earth dam design with 1-m displacement. However, the corresponding values have been commonly used for the stability assessment of natural slopes with an acceptable displacement of 0.05–0.30 m. This could be considered one of the key issues of PS stability analysis of natural slopes [3].

Meanwhile, this PS coefficient value is just an approximation of the complex real ground motion time series for practical slope stability

* Corresponding author.
E-mail address: pooneh.shahmalekpoor.19@ucl.ac.uk (P. Shah Malekpoor).

https://doi.org/10.1016/j.soildyn.2024.108846
Received 12 February 2024; Received in revised form 21 June 2024; Accepted 9 July 2024
Available online 16 July 2024

Table 1
PS coefficients from different studies (after [3]).

Investigator	Recommended PS coefficient (K_h)	Recommended factor of safety (FS)	Calibration conditions
Terzaghi (1950)	*0.1 (R–F[a]=IX)* *0.2 (R–F = X)* *0.5 (R–F > X)*	*>1.0*	*Unspecified*
Seed [4]	*0.10 (M[b] = 6.50)* *0.15 (M = 8.25)*	*>1.15*	*<1 m displacement in earth dams*
Marcuson [2]	*(0.33-0.50) *PGA[c]/g*	*>1.0*	*Unspecified*
Hynes-Griffin and Franklin [5]	*(0.50*peak bedrock acceleration)/g*	*>1.0*	*<1 m displacement in earth dams*
California Division of Mines and Geology [6]	*0.15*	*>1.1*	*Unspecified; probably based on <1 m displacement in dams*

[a] R–F is Rossi-Forel earthquake intensity scale.
[b] M is the earthquake magnitude.
[c] Amplified version of the peak bedrock acceleration measured at a critical point like the crest of the dam.

analysis. Although extensive studies have been conducted to establish the rule of the PS coefficient selection, no consensus is reached for this problem (as seen in Table 1). Thus, employing the uncertainty levels of the PS coefficient is investigated in the literature [7–10], as it is difficult to select a unique constant value for this.

In this regard, a probabilistic distribution is assigned to the PS coefficient. Youssef Abdel Massih et al. (2008) employed the randomness of the horizontal PS coefficient (i.e. employing an exponential distribution as well as an extreme value type II distribution with COV_{Kh} levels of 0.1–0.8) in the reliability analysis of a strip footing subjected to a vertical load. It was shown that for higher values of the applied load, the effect of the random variability of the seismic load was significant. The uncertainty of the seismic demand (i.e. PS horizontal acceleration) was considered in the development of fragility curves of a characteristic geostructure by Tsompanakis et al. [8] using a lognormal distribution with a COV_{Kh} level of 0.1. Johari et al. [9] developed a probabilistic model of seismic slope stability based on Bishop's method using an exponential probability density function for the PS coefficient with COV_{Kh} level of 1. In a later study, Li et al. [10] explored the effect of different levels of the PS coefficient variability, 0.25–0.3, in 3D homogeneous slope stability analysis through employing the limit analysis considering normal and lognormal distribution types. Shah Malekpoor and Lopez-Querol [11] put forward the application of the random fields in modelling the PS loading spatial variability. Later, Shah Malekpoor et al. [12] explored the effect of the PS loading spatial variability on stochastic soil slope stability analysis.

On the other hand, soils vary spatially as a result of depositional and post-depositional processes that entail not constant properties in the space, which is called the soil inherent variability. Such phenomena can be modelled through the theory of random fields [13]. Constraining the random fields to stationary Gaussian ones (even some non-Gaussian e.g. lognormal fields can simply be derived from Gaussian ones) equips the researchers with easy-to-model stochastic fields that require the least number of inputs including the mean value and coefficient of variation (COV) of the soil property, the type of the probabilistic distribution of that property (e.g. normal, lognormal) and the auto-correlation function (ACF) model which represents the correlation relationship between residual components of the same property within the field [14].

Employing the soil spatial variability within the slope reliability analyses is a quite extended approach under different numerical schemes, including random finite difference method (RFDM), random finite element method (RFEM) and circular and non-circular random limit equilibrium method (RLEM). As an example, the effect of anisotropic spatial variability of undrained shear strength in reliability analysis of clay slopes was investigated by Jamshidi Chenari and Alaie [15] through an RFDM approach considering both stationary and non-stationary random fields (RFs) generated by covariance matrix decomposition method. Burgess et al. [1] employed the random field theory and MC simulation together with the finite element method as the slope stability assessment technique (this combination is called RFEM), where the slope failure benchmark was the non-convergence within 500 iterations. However, the high computational effort required in the strength reduction technique makes RLEM more efficient than RFEM, being discussed next [16].

The combination of random fields, Monte Carlo simulations, and circular LEM termed 2D-RLEM was first introduced by Javankhoshdel et al. [17]. Here, the stochastic soil values within the field are generated using the LAS method by Fenton and Vanmarcke [18] and assigned to the soil elements of a slope model for each MC iteration. In fact, the elemental values intersecting the slice base midpoints are considered the soil properties for that slice. Then, the critical slip surface is assessed through the factor of safety, FS value (calculated by one of the limit equilibrium methods of slices) of different surfaces in each MC iteration. In fact, the slip surface with the lowest safety factor is determined at the end of each iteration and its critical value (FS) is compared to one. The probability of failure is finally calculated as the number of iterations with a safety factor less than one to the total number of iterations. Javankhoshdel and Bathurst [19] and Javankhoshdel et al. [17] utilized the circular-RLEM to investigate the influence of soil spatial variability on the slope probability of failure.

Non-circular RLEM was first used by Cami et al. [16] where the Morgenstern-Price method was employed as the slope stability analysis approach combined with the Auto Refine search method, together with the Monte Carlo technique or 'random walking' as the optimization procedure in locating the low-safety-factor non-circular surfaces. It was shown that their non-circular RLEM approach was able to find the weakest failure path, similarly to the failure path using the RFEM approach, though being much more computationally efficient (i.e. 40 % less time). Shah Malekpoor et al. [20] discussed the effect of the mesh size of the soil random fields and the cross-correlation between the strength parameters among other factors in stochastic slope stability analysis using noncircular-RLEM and compared the results with those of Burgess et al. [1] from RFEM. Mafi et al. [21] introduced the surface altering optimization (SAO) method and provided a comprehensive review of the literature on searching methods of critical non-circular slip surfaces (e.g. Monte Carlo optimization among local optimization methods and the cuckoo search and particle swarm optimization among global non-circular search methods) in probabilistic slope stability analysis. It was demonstrated that SAO is a computationally efficient and fairly accurate method of optimising non-circular slip surfaces. In the realm of reinforced soil slopes, Dastpak et al. [22] compared the probabilistic and the stochastic results of noncircular and circular RLEM for the internal and external failure mechanisms.

However, the application of the uncertainty of the PS coefficient in the spatially variable soil slopes has yet to be considered being the focus of the current study. In this regard, the safety margins of the PS approach have been presented through employing the novel stochastic approach presented in Shah Malekpoor et al. [23], which considers the spatially variable attributes for slope stability analyses, i.e. soil properties, and the random variability of the PS coefficient as the critical achievement of the current paper. In fact, the observed trends and turning points in the design aids reported in that research are justified hereinafter to be dependent of the deterministic PS factor of safety range.

As the real-world application in probabilistic slope designs (depending on the target probability of failure), this research shows that there is significant difference between the failure probability of spatially-variable slopes for a constant PS loading approach and considering the uncertainty levels in the PS coefficient even in stable slopes. This aspect should be taken into account by the designers and

analysers.

This paper is organized as follows: the introduction and background on this topic is presented first, followed by the description of the numerical model, geometry, soil conditions and input loading. The main results of the analyses, in the form of design aids, are presented and discussed next. The paper concludes with the main conclusions and recommendations for future work.

2. Methodology

To study the random variable moderate pseudo-static input motions in the stochastic slope stability problem, the Janbu-simplified LEM (to consider non-circular-shape slip surfaces) is employed in the Monte Carlo simulation and random fields to model the spatially variable soil properties. In fact, each Monte Carlo iteration considers a distinct value of the PS coefficient while a random field is generated for the soil parameters per iteration. As the probabilistic approach, this technique uses Monte Carlo simulation (to estimate the slope probability of failure) due to the numerous random variables in the field.

This approach which is called 2D-RPSLEM makes the simulations more realistic while retaining the time efficiency feature of seismic slope stability analyses through the PS approach and limit equilibrium analysis.

The slopes explored in the current study are cohesive-frictional, with a single layer/material and a simplified geometry shown in Fig. 1 where H is the slope height, L represents the slope length, β means the slope angle and D is the depth factor (i.e. The depth factor is simply taken as the depth to the hard layer divided by the height of the slope).

The main aim is to focus on the effect of the random variability of the PS loading using this methodology rather than studying a complex setup of geometry and material. To be more conservative, no cross-correlation is considered between the random variables and the pore pressure is ignored as well.

The mean magnitude of the PS coefficient with lognormal distribution assumption is limited to 0.3 in the current study. In fact, Baker et al. (2006) asserted that the use of the PS approach should be limited to scenarios where the PS coefficient, K_h is below 0.3. The range of COV values considered in the current study for the PS coefficient are assumed to be (0.1–4) which is also similar to the range employed in literature (e.g. Youssef Abdel Massih et al., 2008; [8–10]).

Soil parameters are assumed to follow a lognormal distribution as well according to their nonnegative nature [17,24] and the Markovian ACF, stated before, has been used in the simulations of the random fields. The deterministic and statistical parameter values include $H = 5$ & $10\ m$, $D = 2$, soil unit weight, $\gamma = 18(kN/m^3)$, horizontal SoF for the soil parameters, $\theta_{c,\phi(Ho)} = 200\ m$, vertical SoF for the soil parameters, $\theta_{c,\phi(V)} = 1.5$ & $5\ m$ [1,25,26]. Isotropic fields for the soil parameters are used when it is announced under the figure (e.g. $\theta_{c,\phi(H,V)} = 5\ m$ in Fig. 2); otherwise, anisotropic fields are employed.

The stochastic values for the soil properties (i.e. cohesion and friction angle) are generated by employing the random field theory and local average subdivision method (LAS). These random field values are obtained with the modified RFEM code of Luo et al. [27] which was originally the developed mrslope2d code by Griffiths and Fenton [28]. These stochastic values are then imported into the authors' homemade code as the elemental grid values in the slope where each soil element is assigned a specific cohesion and friction angle considering a distinct PS coefficient value at each MC iteration. The midpoint of the base of each slice is located element-wise, and the corresponding random values are then assigned to the whole slice, leading to the calculations of the factor of safety for that slip surface. The noncircular slip surfaces are generated from the circular ones as is defined by the Auto Refine search method in Slide2 [29]. The final probability of failure is computed as the number of iterations with the resulting minimum factor of safety less than 1 to the total number of iterations.

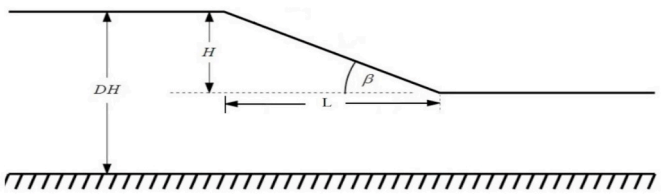

Fig. 1. Sample slope section (after [1]).

The validation of the methodology was conducted by comparing the results with Slide2 [29] software for some cases (when the PS loading is non variable) considering different factors including the optimal number of slices, surfaces and the similarity of the mechanism of failure. The optimal number of slices (which also is representative of the optimal slice width) and surfaces were determined based on comparing the minimum factor of safety values from the code with Slide2 results, using the same input random field when the soil is stochastic, but the PS coefficient is taken as constant. It is observed that the minimum factor of safety does not change significantly after considering more than 100 slices and 20,000 surfaces which was also confirmed by Slide2. Moreover, the mesh size of the random fields is chosen according to the smallest SoF value used. Huang and Griffiths (2015) recommended using a mesh size of less than half of the correlation length (or SoF), e.g. 0.5 m*0.5 m when SoF is 1.5 m. In a later research, Chu et al. (2016) showed that the ratio of mesh size to the SoF should be confined to 0.4, here the requirements of the mesh = 0.5 m $\leq$ 1.5*0.4 (0.6) is satisfied.

To make sure of the similarity of the mechanism of failure and the generated random fields from the current method to Slide2, a comparison has been made for two different iterations and the results are shown in Figs. 2 and 3 where two different cohesion random fields are shown together with the critical non-circular slip surfaces resulting from Slide2 and this methodology for two different types of failure mechanisms (i.e. toe failure in Fig. 2 and base failure in Fig. 3). This comparison confirms the validity of the current methodology in terms of the failure mechanism and accurate mapping of the random values in the field as well.

A comparison has also been conducted between the resulting critical circular and noncircular surfaces for two iterations which shows the more critical output (i.e. minimum safety factor) of the Janbu-simplified (Figs. 4 and 5).

A flowchart has been shown in Fig. 6 which describes the procedure in developing this methodology. Finally, a different number of MC samples were tried to find the optimal number of samples (in terms of time and accuracy) for this type of analysis. It was observed that 2000 samples were enough for all failure probabilities (Figs. 7 and 8), as a higher number of iterations does not have a significant influence on the probability of failure.

3. Results and discussion

As previously mentioned, the methodology newly developed and presented in the previous sections of this paper is employed to reflect more realistic outputs as it considers the random variability of the input motion. This method is employed to investigate the effect of different mean values and uncertainty levels of the single random variable PS coefficient and the soil vertical spatial variability on the probability of failure of the theoretical stochastic slopes. The results have been presented in this section.

As expected, an elevation in the stability number, signifying higher soil cohesion while maintaining a constant slope height and friction angle, results in a diminished probability of failure (i.e. increased deterministic factor of safety) for a given slope angle under random variable PS loading. Conversely, an increased mean magnitude for the PS coefficient is associated with a heightened risk of failure for a specific slope as this reduces the safety level of the slope (refer to Figs. 9 and 10).

Fig. 9 illustrates that varying levels of uncertainty in the horizontal PS coefficient minimally impact the vulnerability of a stochastic slope at

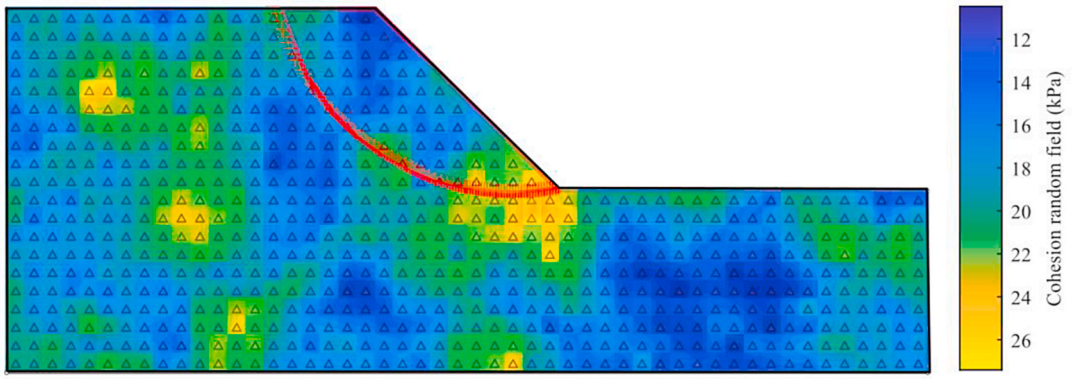

Fig. 2. Mapped results with $\beta = 45^{\circ}$, $H = 10$ m, $K_h = 0.1$(constant), $\mu_c = 16$(kPa), $\mu_\phi = 20^{\circ}$, $COV_c = COV_\phi = 0.2$, $\theta_{c,\phi(H,V)} = 5$, RF1 (solid curve: Slide2 with $FS_{min} = 1.017$, plus curve: this study with $FS_{min} = 1.0598$).

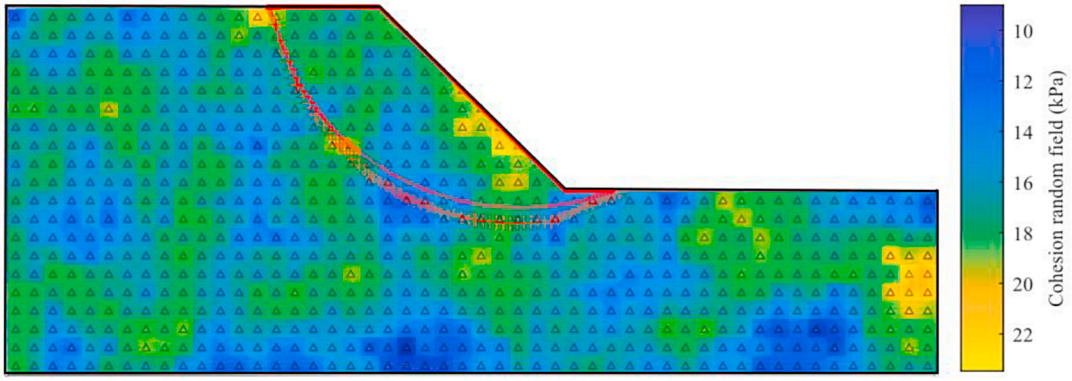

Fig. 3. Mapped results with $\beta = 45^{\circ}$, $H = 10$ m, $K_h = 0.1$(constant), $\mu_c = 16$(kPa), $\mu_\phi = 20^{\circ}$, $COV_c = COV_\phi = 0.2$, $\theta_{c,\phi(H,V)} = 5$ m, RF2 (solid curve: Slide2 with $FS_{min} = 0.956$, plus curve: this study with $FS_{min} = 0.9468$).

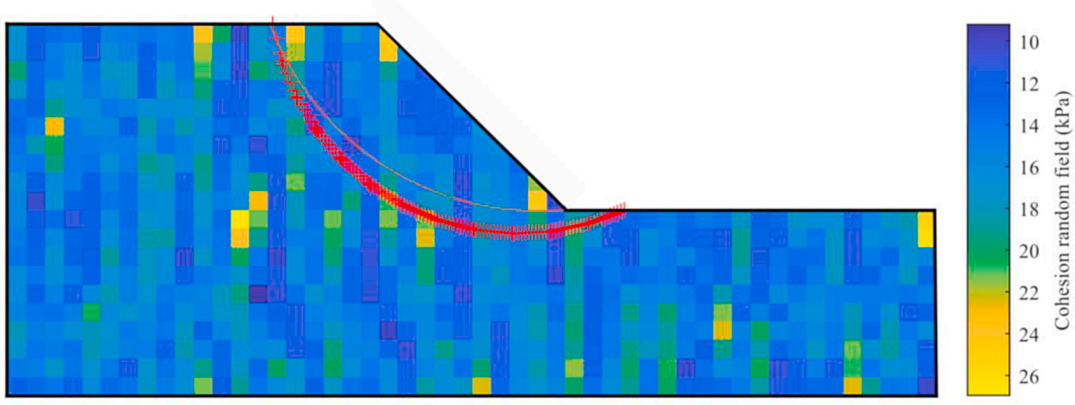

Fig. 4. Comparison between the circular and noncircular mechanisms with $\beta = 45^{\circ}$, $H = 10$ m, $K_h = 0.1$(constant), $\mu_c = 16$(kPa), $\mu_\phi = 20^{\circ}$, $COV_c = COV_\phi = 0.2$, $\theta_{c,\phi(H,V)} = 5$ m, RF4 (solid circular curve with FS (Bishop) = 1.1, non-circular plus-line curve with FS (Janbu simplified) = 0.95).

low mean input load levels ($\mu_{Kh} = 0.1$). However, this aspect becomes significantly crucial at higher loads for all slope angles, as depicted in Fig. 10. This can be justified through the low standard deviation values resulting from low mean magnitudes of the PS coefficient, thus different simulations (considering different COV_{Kh} levels) do not hold significant differences in results (Fig. 9).

For both mean PS coefficient values (i.e., $\mu_{Kh} = 0.1$ and 0.3), the critical or worst-case COV_{Kh} value, leading to a higher probability of slope failure compared to other COV_{Kh} values, transitions from 0.1 to 0.5 for slopes with a risk of failure below approximately 40 %. For instance, in the case of a slope with a high stability number ($\lambda = 0.7$), increasing the mean value of the PS coefficient to 0.3 results in much higher probabilities of failure for COV_{Kh} equal to 0.5 when compared to a constant K_h approach (see Fig. 10). This matter can be explained through the safety factor approach in Figs. 11–13.

It is worth noting that the constant K_h approach (i.e., no uncertainty in the input load) exhibits a compatible trend with the curves representing different uncertainty levels (ranging from $COV_{Kh} = 0.1$ to $COV_{Kh} = 0.5$) (refer to Figs. 9 and 10). The Janbu simplified PS safety factor is also accessible through these two charts for a range of slope angles. In

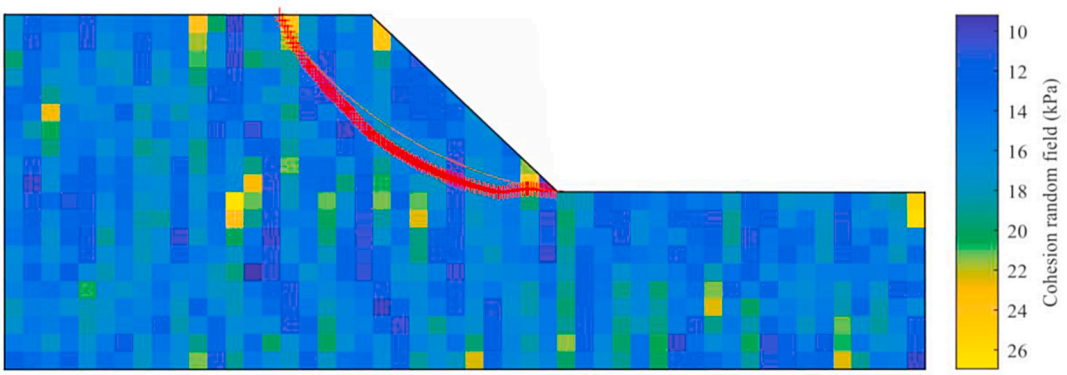

Fig. 5. Comparison between the circular and noncircular mechanisms with $\beta = 45^{\circ}$, $H = 10$ m, $K_h = 0.1$(constant), $\mu_c = 16$(kPa), $\mu_\phi = 20^{\circ}$, $COV_c = COV_\phi = 0.2$, $\theta_{c,\phi(H,V)} = 5$ m, RF11 *(solid circular curve with FS (Bishop) = 0.99, non-circular plus-line curve with FS (Janbu simplified) = 0.94).*

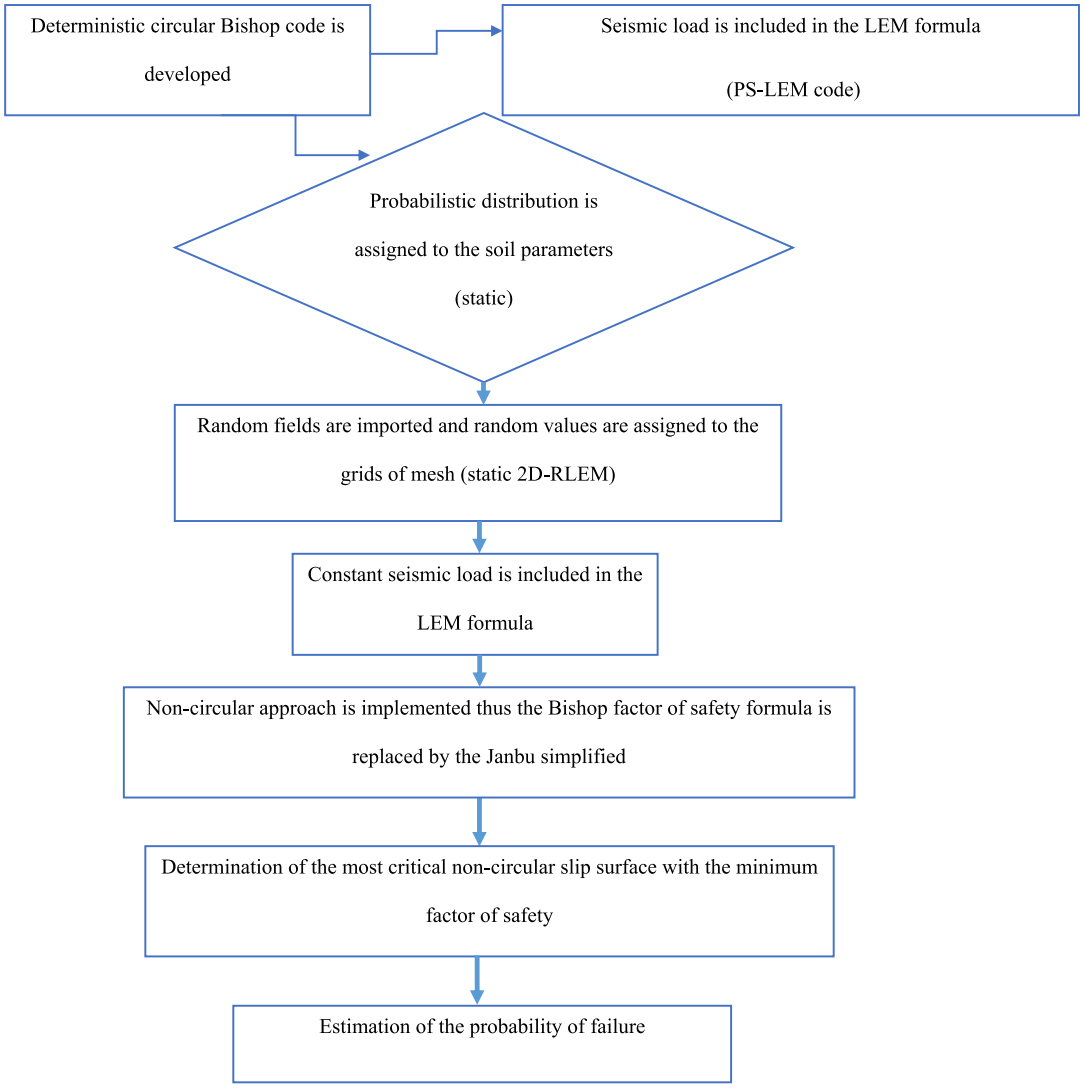

Fig. 6. Flowchart of the procedure in developing the methodology.

fact, PS factor of safety of a slope with $\beta = 40^{\circ}$, $\lambda = 0.3$, $\mu_\phi = 20^{\circ}$, and $\mu_{Kh} = 0.1$ (deterministic parameter values) is 1.14 which is shown by the green arrow pointing to the right in Fig. 9. On the other hand, the pointing to the left green arrow in the same figure represents the probability of failure for this slope in a spatially variable context with statistical parameters mentioned in the caption and is estimated to be 9.8 % when COV_{Kh} is 0.5.

Another representation of the results will be discussed here with respect to both mean magnitude of 0.1 and 0.3 for the PS coefficient. To include a variety of range of slope inclinations, the effect of different levels of the random variability of the PS coefficient has been explored considering different levels of COV_{Kh} (i.e. 0.2, 0.5 and 4 as justified

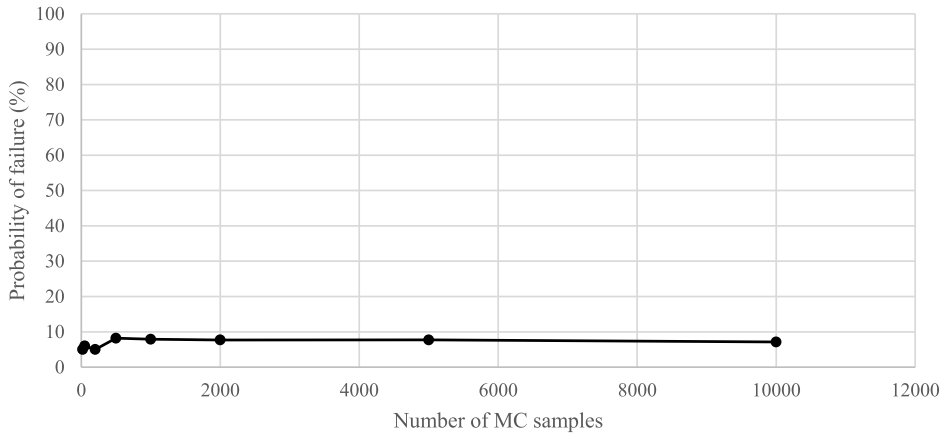

Fig. 7. Optimal number of MC samples for P_f under 10 % (assuming $\beta = 20^{\circ}$, $\mu_{\phi} = 20^{\circ}$, $\lambda = 0.9$, $\mu_{Kh} = 0.3$, $H = 5$ m, $\gamma = 18$ kN/m3, $COV_c = 0.3$, $COV_{\phi} = 0.15$, $COV_{Kh} = 0.5$, $(\theta_{c,\phi})_{Ho}/H = 40$, $(\theta_{c,\phi})_V/H = 0.3$).

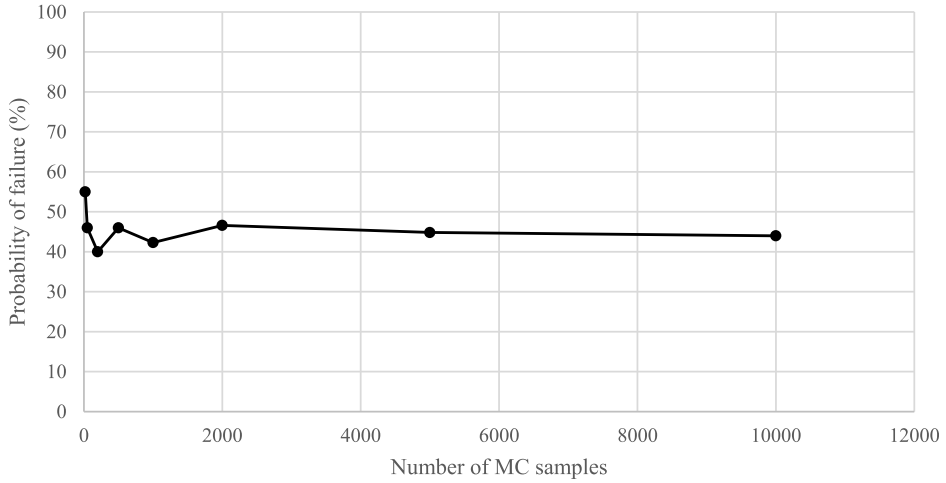

Fig. 8. Optimal number of MC samples for P_f over 10 % (assuming $\beta = 20^{\circ}$, $\mu_{\phi} = 20^{\circ}$, $\lambda = 0.3$, $\mu_{Kh} = 0.3$, $H = 5$ m, $\gamma = 18$ kN/m3, $COV_c = 0.3$, $COV_{\phi} = 0.15$, $COV_{Kh} = 0.5$, $(\theta_{c,\phi})_{Ho}/H = 40$, $(\theta_{c,\phi})_V/H = 0.3$).

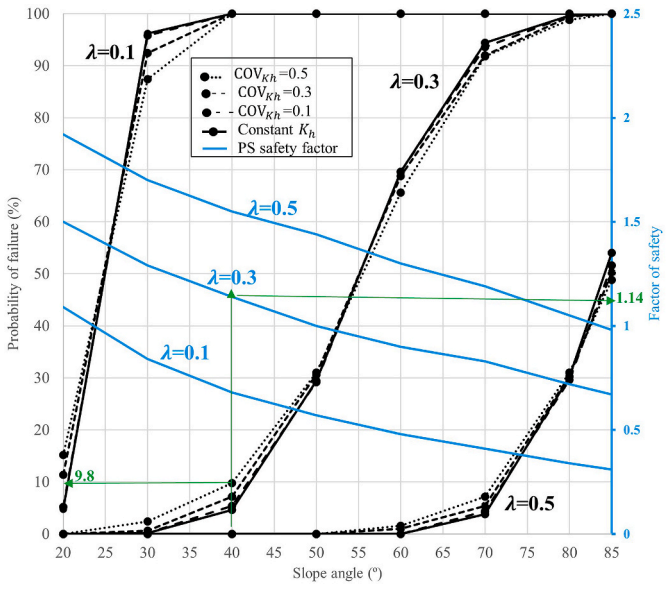

Fig. 9. The effect of various levels of COV_{Kh} and λ for $\mu_{Kh} = 0.1$, $\mu_{\phi} = 20^{\circ}$, $COV_c = 0.3$, $COV_{\phi} = 0.15$, $(\theta_{c,\phi})_{Ho}/H = 40$, $(\theta_{c,\phi})_V/H = 0.3$ with a Markovian ACF.

before) for mild, medium and steep slope geometries (i.e. 20°, 40° and 60°). Uncertainty levels in the determination and choice of K_h in preliminary stages of seismic design for slopes with PS factors of safety above around 1.1 show unconservative behaviour of the constant K_h approach for all slope angles and both mean magnitudes of the PS coefficient (Figs. 11–17). In fact, the higher the value of the deterministic PS safety factor, the more critical is a higher level of the uncertainty and a staged pattern in P_f corresponding to different levels of the COV of the PS coefficient is observed in the following graphs (Figs. 11–17). This can be interpreted as different worst-case COV_{Kh} levels for different ranges of the deterministic PS safety factors (or different ranges of probability of failure). For example, green arrows in Fig. 14 show that a constant level of the PS coefficient leads to a probability of failure of 15.2 %, while uncertainty levels of 0.2, 0.5 and 4 result in 27.2 %, 30.4 % and 17 % corresponding to a PS safety factor of 1.12 (thus the worst-case COV is 0.5 for this safety factor). The red rectangular boxes in Figs. 11–17 indicate the range of PS deterministic safety factor of slopes where a constant approach is unconservative. This matter underlines the importance of considering different levels of the PS uncertainty in probabilistic seismic slope stability designs. This also explains the trends in Figs. 9 and 10 where the worst case COV levels of the PS coefficient changes by increasing the slope angle (i.e. lowering the factor of safety). In fact, a constant approach corresponds to higher probabilities of failure compared to other COV levels for slopes with safety factors less than about 1.1 while a high variability level for the PS coefficient is the worst-

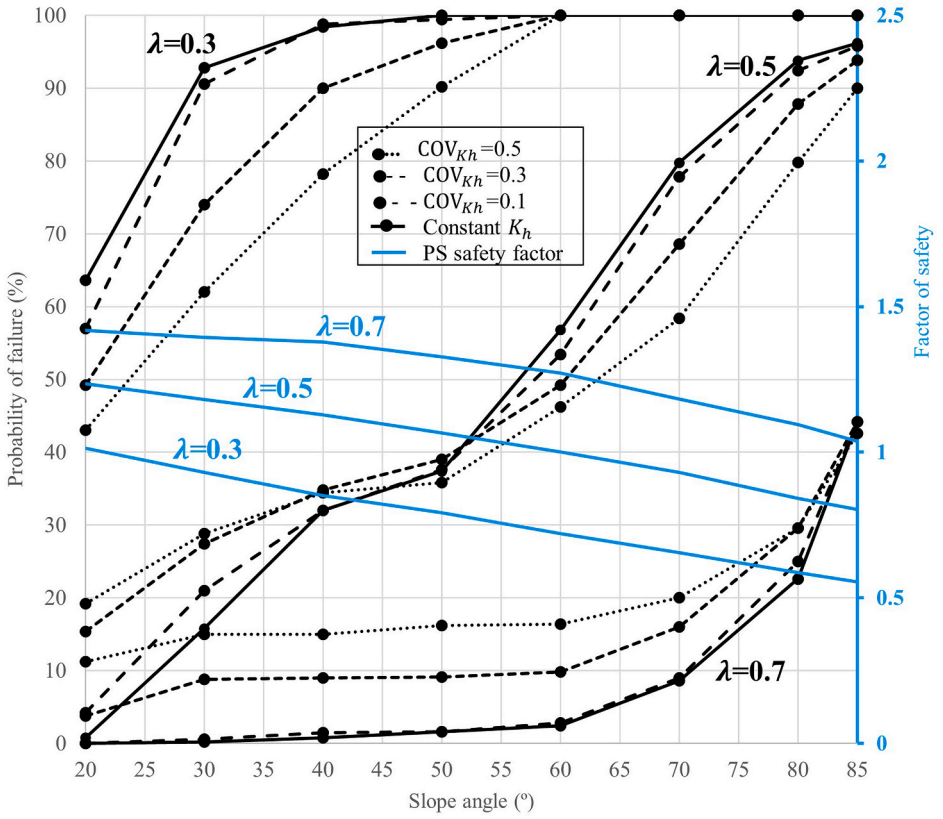

Fig. 10. The effect of various levels of COV_{Kh} and λ for $\mu_{Kh} = 0.3$, $\mu_{\phi} = 20°$, $COV_c = 0.3$, $COV_{\phi} = 0.15$, $(\theta_{c,\phi})_{Ho}/H = 40$, $(\theta_{c,\phi})_V/H = 0.3$ with a Markovian ACF.

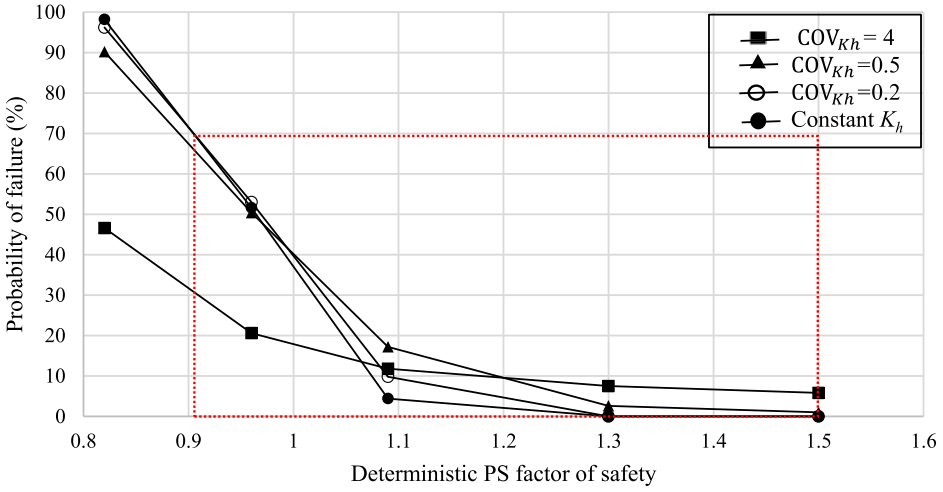

Fig. 11. Comparison between deterministic and probabilistic seismic approaches ($\beta = 20°$, $H = 5$ m, $\mu_{Kh} = 0.1$, $COV_c = 0.3$, $\mu_{\phi} = 20°$, $COV_{\phi} = 0.15$, $(\theta_{c,\phi})_{Ho}/H = 40$, $(\theta_{c,\phi})_V/H = 0.3$).

case scenario for slopes with higher safety factor levels explaining the turning points in previous design aids (Figs. 9 and 10).

Totally, a constant approach is not safe and reasonable for slopes with certain ranges of the deterministic PS factors of safety in moderate seismic areas with PS coefficients of 0.1 and 0.3. It is vital to consider different uncertainty levels of the PS coefficient and choose the suitable graph among others considering the slope angle, the value of the PS coefficient and the slope PS safety factor (Figs. 11–17). Considering this limitation of the constant approach (i.e. uncertainty in the PS coefficient value) can serve as a better seismic probabilistic design of the slopes e.g. Fig. 15 which shows that for a slope with deterministic safety factor of 1.37, a constant approach yields a desirable close to 0 probability of failure while an uncertainty level of 0.2 leads to the P_f of 7 %. Importantly, Fig. 17 confirms the broader relevance of the results considering a higher slope.

To observe the effect of the soil vertical spatial variability on the results, a longer value (i.e. 5 m) has also been tried as the vertical spatial correlation length of the soil as the soil is expected to have a lower correlation length in the vertical direction (i.e. anisotropic behaviour in real), thus the effect of the horizontal variation can be discarded. The analyses have been repeated for three different levels of the COV of the PS coefficient in addition to the constant approach. As it can be

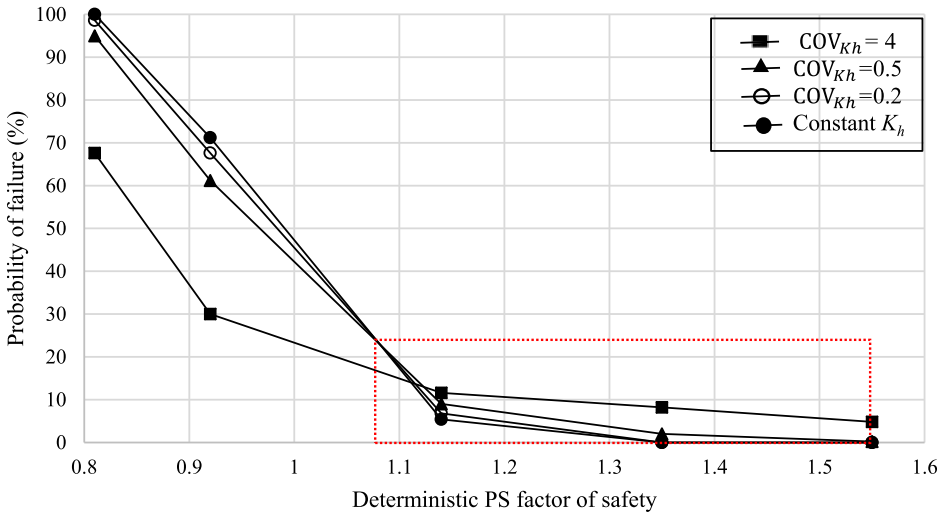

Fig. 12. Comparison between deterministic and probabilistic seismic approaches *($\beta = 40°$, $H = 5$ m, $\mu_{Kh} = 0.1$, $COV_c = 0.3$, $\mu_\phi = 20°$, $COV_\phi = 0.15$, $(\theta_{c,\phi})_{Ho}/H = 40$, $(\theta_{c,\phi})_V/H = 0.3$).*

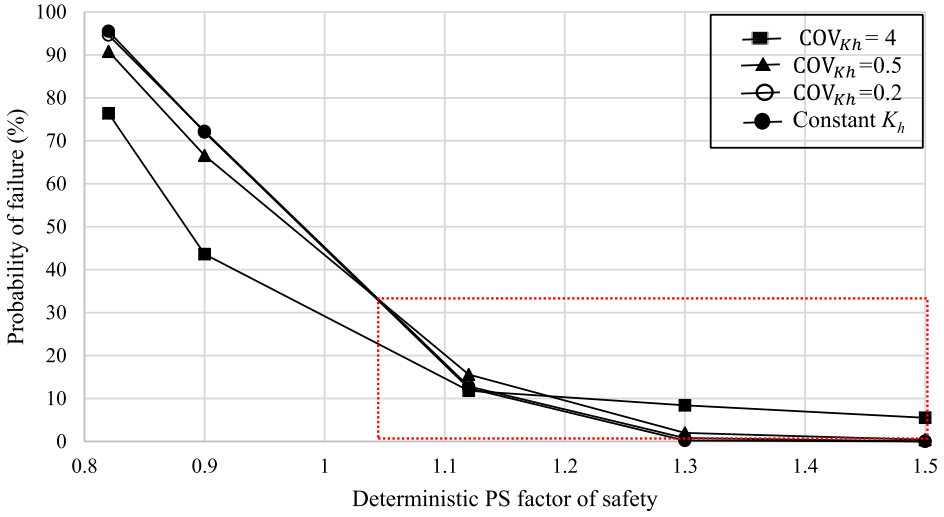

Fig. 13. Comparison between deterministic and probabilistic seismic approaches *($\beta = 60°$, $H = 5$ m, $\mu_{Kh} = 0.1$, $COV_c = 0.3$, $\mu_\phi = 20°$, $COV_\phi = 0.15$, $(\theta_{c,\phi})_{Ho}/H = 40$, $(\theta_{c,\phi})_V/H = 0.3$).*

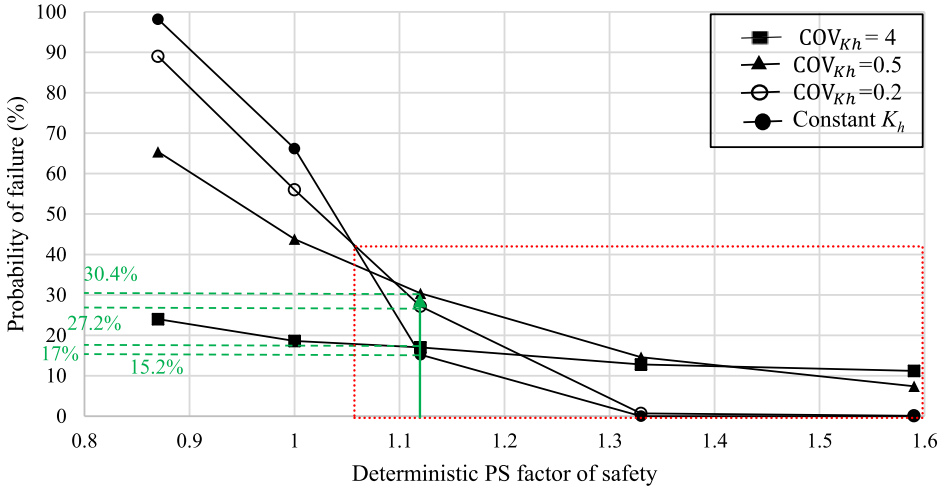

Fig. 14. Comparison between deterministic and probabilistic seismic approaches *($\beta = 20°$, $H = 5$ m, $\mu_{Kh} = 0.3$, $COV_c = 0.3$, $\mu_\phi = 20°$, $COV_\phi = 0.15$, $(\theta_{c,\phi})_{Ho}/H = 40$, $(\theta_{c,\phi})_V/H = 0.3$).*

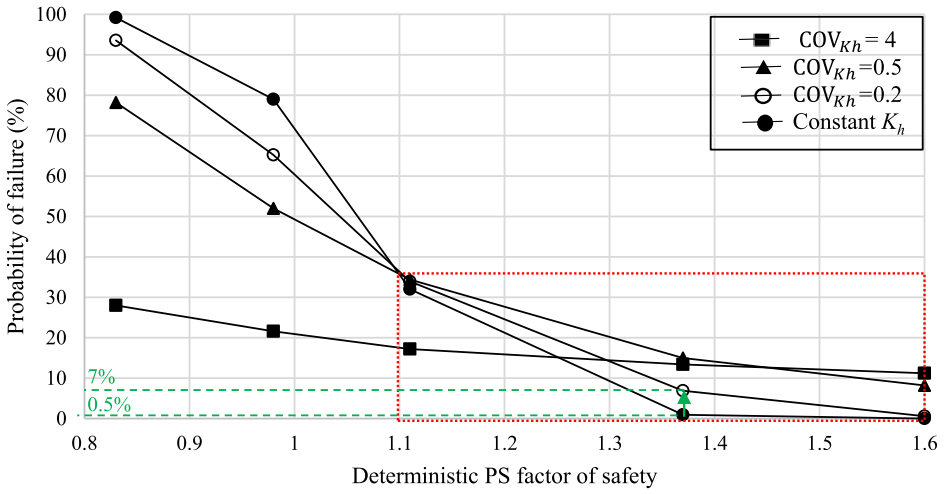

Fig. 15. Comparison between deterministic and probabilistic seismic approaches *($\beta = 40°$, $H = 5$ m, $\mu_{Kh} = 0.3$, $COV_c = 0.3$, $\mu_\phi = 20°$, $COV_\phi = 0.15$, $(\theta_{c,\phi})_{Ho}/H = 40$, $(\theta_{c,\phi})_V/H = 0.3$).*

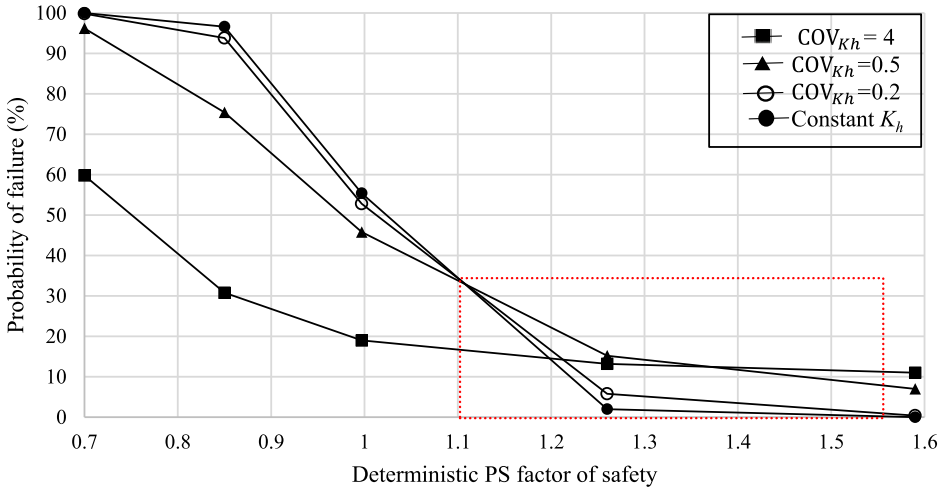

Fig. 16. Comparison between deterministic and probabilistic seismic approaches *($\beta = 60°$, $H = 5$ m, $\mu_{Kh} = 0.3$, $COV_c = 0.3$, $\mu_\phi = 20°$, $COV_\phi = 0.15$, $(\theta_{c,\phi})_{Ho}/H = 40$, $(\theta_{c,\phi})_V/H = 0.3$).*

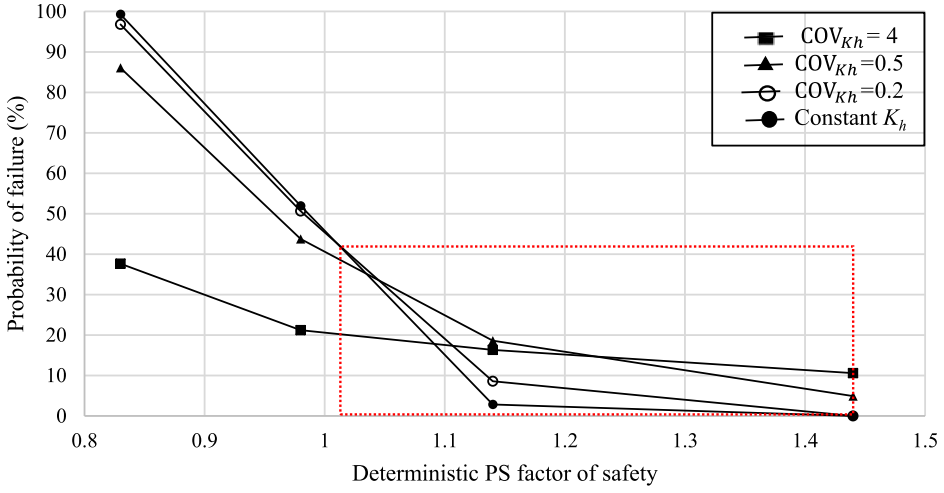

Fig. 17. Comparison between deterministic and probabilistic seismic approaches *($\beta = 45°$, $H = 10$ m, $\mu_{Kh} = 0.2$, $COV_c = COV_\phi = 0.2$, $\mu_\phi = 20°$, $(\theta_{c,\phi})^{11}{}_{(H,V)}/H = 0.5$).*

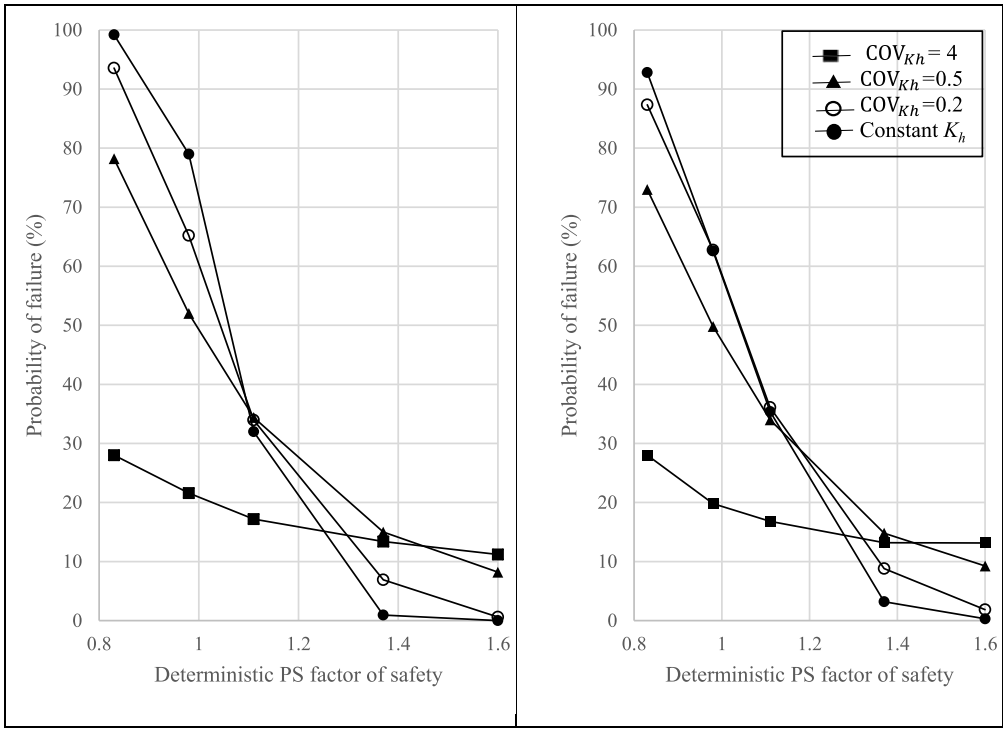

Fig. 18. The effect of different vertical spatial variability level of the soil ($\beta = 40^{\circ}$, $H = 5$ m, $\mu_{Kh} = 0.3$, $COV_c = 0.3$, $\mu_{\phi} = 20^{\circ}$, $COV_{\phi} = 0.15$, $(\theta_{c,\phi})_{Ho}/H = 40$, $(\theta_{c,\phi})_V/H = 0.3$ (left), $(\theta_{c,\phi})_V/H = 1$(right)).

observed, a greater vertical correlation length for the soil led to minimal changes in the results, especially the trend is similar (Fig. 18).

4. Conclusion

This research includes a novel viewpoint towards the PS approach in seismic stochastic slope stability analyses. The methodology employed, i.e. 2D- RPSLEM, asserts the necessity of considering various levels of COV of the PS coefficient as it is shown that there is a disparity between the results when adopting different values as the COV of the seismic input load. In this regard, theoretical slope models have been analysed to understand the influence of the different levels of input motion and its uncertainty levels. The most important conclusions derived from this research are listed next.

1. Uncertainty of the seismic load plays a bolder role for higher mean magnitude of the PS coefficients (or higher PGA values).
2. It is routine to apply a constant PS load in probabilistic slope stability analyses according to previous references. This method is justifiable and safe for slopes with FS less than about 1.1 (failure probabilities above about 40 %). However, this approach is unrealistic as different researchers have presented different relationships for the calculation of the PS coefficient, thus showing great uncertainty for its value. More importantly, it has been shown that this constant approach may have an unconservative performance for deterministic PS safety factors above 1.1 or failure probabilities less than about 30 % for all slope angles and PS coefficient values investigated in the current research. Thus, different uncertainty levels of the PS coefficient must be taken into account for such slopes.
3. This research shows a significant difference between the failure probability of spatially-variable slopes for a constant PS loading approach and considering the uncertainty levels in the PS coefficient value even in stable slopes (for both mean PS coefficient values of 0.1 and 0.3). This difference in the failure probability should be considered by the designers who consider a target probability of failure.
4. Analysis of a higher slope (10 m) has led to similar trends and confirmed the constant PS approach being unconservative for slopes with deterministic safety factors above around 1.1. This shows the broad relevance of the PS approach safety margins and this research results in engineering practice.
5. The soil vertical spatial variability does not have a significant influence on the boundary value deterministic PS safety factor (i.e. 1.1).
6. The difference between the results due to different uncertainty levels of K_h is found to be more significant for lower safety factors or when the slope is highly vulnerable.
7. The worst case COV_{Kh} value (which results in the greater vulnerability of the stochastic slope or a higher probability of failure compared to other COV_{Kh} values) changes from 0.2 to 4 for all slope angles and soil vertical spatial variability values as the safety factor increases.

This matter might revolutionize the applications of the PS approach in the realm of seismic probabilistic slope stability analysis as the routine might compromise the safety of the design for specific slopes (with PS safety factor above around 1.1) in seismic regions of the world. It is suggested to consider the effect of the cross-correlation between the soil parameters, the existence of different soil profiles within the slope geometry as well as the pore pressure effect in future research studies. Importantly, this revolutionary methodology is the first step to the development of a complete set of design charts which require further analyses of different geometries and soil types.

CRediT authorship contribution statement

Pooneh Shah Malekpoor: Writing – original draft, Validation, Resources, Methodology, Investigation, Conceptualization. **Susana Lopez-Querol:** Supervision, Project administration. **Sina Javankhoshdel:**

[1] Isotropic correlation length of the cohesion and friction angle random field.

Supervision, Software.

Declaration of competing interest

The authors declare that they have no known competing financial interests or personal relationships that could have appeared to influence the work reported in this article.

Please note.

This declaration of interest statement must be uploaded as a separate file in the submission system.

- The corresponding author must complete this form on behalf of all the authors of a submission.
- Please ensure that this is done.

Data availability

No data was used for the research described in the article.

Acknowledgements

The corresponding author wishes to acknowledge the gracious Fund Award received from the BGA (British Geotechnical Association). The authors would like to thank Rocscience Inc. for providing them with the computational tools.

References

[1] Burgess J, Fenton GA, Griffiths DV. Probabilistic seismic slope stability analysis and design. Can Geotech J 2019;56(12):1979–98. https://doi.org/10.1139/cgj-2017-0544.
[2] Marcuson WF. Moderator's report for session on earth dams and stability of slopes under dynamic loads. In: International conference on recent advances in geotechnical earthquake engineering and soil dynamics. vol. 3; 1981. p. 1175. St. Louis, MO.
[3] Jibson RW. Methods for assessing the stability of slopes during earthquakes- A retrospective. Eng Geol 2011;122(1):43–50. https://doi.org/10.1016/j.enggeo.2010.09.017.
[4] Seed HB. Considerations in the earthquake-resistant design of earth and rockfill dams. Geotechnique 1979;29:215–63.
[5] Hynes-Griffin ME, Franklin AG. Rationalizing the seismic coefficient method. In: Miscellaneous paper GL-84-13. U.S. Army Corps of Engineers Waterways Experiment Station; 1984. p. 37.
[6] California Division of Mines and Geology. Guidelines for evaluating and mitigating seismic hazards in California, vol. 117. California Division of Mines and Geology Special Publication; 1997. p. 74.
[7] Youssef Abdel Massih D, Soubra AH, Low BK. Reliability-based analysis and design of strip footings against bearing capacity failure. J Geotech Geoenviron Eng 2008;134(7). https://doi.org/10.1061/ASCE1090-02412008134:7917.
[8] Tsompanakis Y, Lagaros ND, Psarropoulos PN, Georgopoulos EC. Probabilistic seismic slope stability assessment of geostructures. Structure and Infrastructure Engineering 2010;6(1–2):179–91. https://doi.org/10.1080/15732470802664001.
[9] Johari A, Mousavi S, Hooshmand Nejad A. A seismic slope stability probabilistic model based on bishop's method using analytical approach. Sci Iran 2015;22(3):728–41.
[10] Li D, Sun M, Yan E, Yang T. The effects of seismic coefficient uncertainty on pseudo-static slope stability: a probabilistic sensitivity analysis. Sustainability 2021;13(15). https://doi.org/10.3390/su13158647.
[11] Shah Malekpoor P, Lopez-Querol S. A novel stochastic pseudo-static approach for c–ϕ slopes. Newcastle: 16th Young Geotechnical Engineers Symposium; 2022. July 4-5.
[12] Shah Malekpoor P, Lopez-Querol S, Javankhoshdel S. Spatial variability of input motion in stochastic slope stability. In: Proceedings of the TMIC 2022; 2022. December 12-13.
[13] Vanmarcke EH. Random fields: analysis and synthesis. MIT Press; 1984.
[14] Fenton GA, Griffiths DV. Risk assessment in geotechnical engineering. New Jersey: Wiley; 2008.
[15] Jamshidi Chenari R, Alaie R. Effects of anisotropy in correlation structure on the stability of an undrained clay slope. Georisk 2015;9(2):109–23. https://doi.org/10.1080/17499518.2015.1037844.
[16] Cami B, Javankhoshdel S, Bathurst RJ, Yacoub T. Influence of mesh size, number of slices, and number of simulations in probabilistic analysis of slopes considering 2D spatial variability of soil properties. Proceedings of IFCEE 2018:186–96. Orlando, March 5-10.
[17] Javankhoshdel S, Luo N, Bathurst RJ. Probabilistic analysis of simple slopes with cohesive soil strength using RLEM and RFEM. Georisk 2017;11(3):231–46. https://doi.org/10.1080/17499518.2016.1235712.
[18] Fenton GA, Vanmarcke EH. Simulation of random fields via local average subdivision. J Eng Mech 1990;116(8):1733–49. https://doi.org/10.1061/(ASCE)0733-9399(1990)116:8(1733).
[19] Javankhoshdel S, Bathurst RJ. Simplified probabilistic slope stability design charts for cohesive and cohesive-frictional (c–ϕ) soils. Can Geotech J 2014;51(9):1033–45. https://doi.org/10.1139/cgj-2013-0385.
[20] Shah Malekpoor P, Jamshidi Chenari R, Javankhoshdel S. Discussion of "Probabilistic seismic slope stability analysis and design. Canadian Geotechnical 2020;57(7):1103–8. https://doi.org/10.1139/cgj-2019-0386.
[21] Mafi R, Javankhoshdel S, Cami B, Jamshidi Chenari R, Gandomi AH. Surface altering optimisation in slope stability analysis with non-circular failure for random limit equilibrium method. Georisk 2020:1–27. https://doi.org/10.1080/17499518.2020.1771739.
[22] Dastpak P, Jamshidi Chenari R, Cami B, Javankhoshdel S. Noncircular deterministic and stochastic slope stability analyses and design of simple geosynthetic-reinforced soil slopes. Int J GeoMech 2021;21(9). https://doi.org/10.1061/(ASCE)GM.1943-5622.0002116.
[23] Shah Malekpoor P, Lopez-Querol S, Javankhoshdel S. Stochastic slope stability analysis: exploring the uncertainty of input motion. 2023. RIC2023, Toronto, April 24-26.
[24] Cho SE. Effect of spatial variability of soil properties on slope stability. Eng Geol 2007;92(3–4):97–109. https://doi.org/10.1016/j.enggeo.2007.03.006.
[25] Phoon KK, Kulhawy FH. Characterization of geotechnical variability. Can Geotech J 1999;36(4):612–24. https://doi.org/10.1139/t99-038.
[26] Cami B, Javankhoshdel S, Phoon KK, Ching J. Scale of fluctuation for spatially varying soils: estimation methods and values. ASCE-ASME Journal of Risk and Uncertainty in Engineering Systems Part A: Civil Engineering 2020;6(4):03120002. https://doi.org/10.1061/ajrua6.0001083.
[27] Luo N, Bathurst RJ, Javankhoshdel S. Probabilistic stability analysis of simple reinforced slopes by finite element method. Comput Geotech 2016;77:45–55.
[28] Griffiths DV, Fenton GA. Probabilistic slope stability analysis by finite elements. J Geotech Geoenviron Eng 2004;130(5):507–18. https://doi.org/10.1061/ASCE1090-02412004130:5507.
[29] Rocscience. Slide2, 2D limit equilibrium slope stability software. Toronto, Ontario, Canada: Rocscience; 2023.